

Planar Two-Dimensional Scanning Multibeam Array Antenna Based on a 3×3 Butler Matrix Network

Shu-Kuan Zhao , Miao Lv, Zhi-ya Zhang , Member, IEEE, Qiang Chen , Senior Member, IEEE, and Guang Fu

Abstract—In this letter, a wideband two-dimensional (2-D) scanning multibeam array antenna is proposed using a novel beamforming network (BFN). First, a novel three-beam Butler matrix (BM) network, as the core of the BFN, is proposed and described. The BM network comprises a directional coupler, T-shaped power dividers, and coupling baluns, which avoids using crossovers and lossy lumped elements as in a conventional BM network. In addition, a dual-stripine structure is employed to combine multiple components, which considerably reduces the BM network aperture. Then, six three-beam BMs are stacked and interconnected to form a complete 2-D BFN, whose scanning features of two orthogonal planes are controlled by two sets of BMs. Finally, to verify the working principle of the BFN, a 3×3 all-metal antenna array is designed and combined with the BFN. Notably, the low-profile antenna element achieves a wide operating bandwidth of 34.5%. Furthermore, a prototype is fabricated and tested, which shows that the antenna realizes switched beams in nine directions, indicating that an excellent 2-D scanning function is realized.

Index Terms—Beamforming network (BFN), Butler matrix (BM), multibeam, two-dimensional (2-D) scanning, wideband.

I. INTRODUCTION

WITH the development of smart antenna technology, the multibeam antenna, a core technology, has been widely studied recently. An array antenna with a beamforming network (BFN) can realize multisector coverage that has higher capacity and more flexible operation modes than antennas with single-sector coverage [1]–[3].

For different applications, the Blass matrix [4]–[6], Nolen matrix [7]–[9], and Butler matrix (BM) [10]–[19] networks are commonly employed as BFNs. The application of the BM network in a smart antenna field has been more successful than the other two networks because of its excellent performance in terms of broadband realization, low power loss, and easy realization [10]. In recent years, various BM schemes have been proposed, such as microstrips [11]–[13], striplines [14]–[17],

Manuscript received February 6, 2022; accepted March 12, 2022. Date of publication March 25, 2022; date of current version June 2, 2022. This work was supported in part by the Shaanxi Key Laboratory of Integrated and Intelligent Navigation under Grant SKLIIN-20190101 and in part by the CETC Key Laboratory of Data Link Technology under Grant CLDL-20202413. (Corresponding author: Zhi-ya Zhang.)

Shu-Kuan Zhao, Miao Lv, Zhi-ya Zhang, and Guang Fu are with the National Key Laboratory of Antennas and Microwave Technology, Xidian University, Xi'an 710071, China (e-mail: sk562653807@163.com; superboy-zone@126.com; zhiyazhang@163.com; gfu@mail.xidian.edu.cn).

Qiang Chen is with the Department of Communications Engineering, Tohoku University, Sendai 980-8579, Japan (e-mail: chenq@ecei.tohoku.ac.jp).

Digital Object Identifier 10.1109/LAWP.2022.3160456

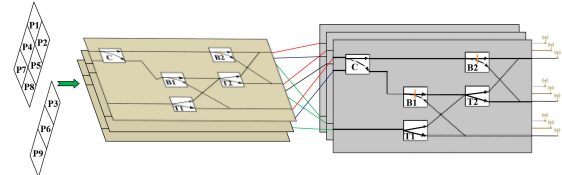


Fig. 1. Topology of the proposed 2-D multibeam array antenna.

waveguides [18], and substrate integrated waveguides [19]. Numerous studies concerning BM networks have focused on circuit miniaturization, bandwidth enhancement, and flexible beams. However, complex crossover junctions and phase shifters are required to expand the bandwidth and flexibly control the beam [13]. In addition, the most common method to achieve a compact structure is to load lumped components [12] or use a costly multilayer structure [14]–[17]. Notably, these flaws limit the use of BMs in various scenarios.

As an extension of a one-dimensional (1-D) scanning phased array, 2-D multibeam antennas have the advantages of wider coverage, higher data transmission rates, and more extensive application scenarios. However, 2-D BFNs usually have large-scale complex circuits, especially planar structures [20]–[25]. The accumulated power loss and the large number of crossovers in the realization make the design challenging. In such a case, the complexity of the circuit can be effectively reduced by cascading 1-D BFNs to achieve 2-D scanning functions [9], [25].

In this letter, a 2-D scanning phased array using a 2-D BFN comprising six novel three-beam BM networks is proposed. The overall topology of the BFN is first provided in Section II. As the core component of the BFN, a compact wideband three-beam BM is introduced and analyzed in detail. To verify the effectiveness of the BFN, a 3×3 array antenna is designed for compatibility with the BFN. Afterward, a prototype is fabricated, tested, and discussed in Section III, which shows that an excellent 2-D scanning function is realized.

II. GEOMETRY AND WORKING PRINCIPLE

The topology of the proposed 2-D scanning multibeam array antenna is shown in Fig. 1. The novel three-beam BM has three output ports that can provide constant amplitude and three phase delays of -120° , 120° , and 0° when the three input ports are individually excited. Six three-beam BMs of the BFN are divided into two groups and stacked together to manipulate the beam direction of two orthogonal directions. Moreover, by switching between the input port excitation, nine beams with

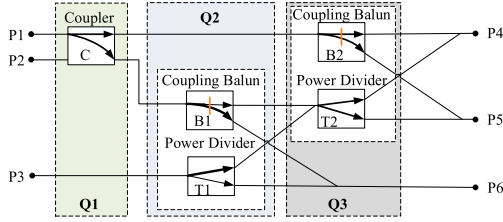


Fig. 2. Topology of the proposed three-beam BM.

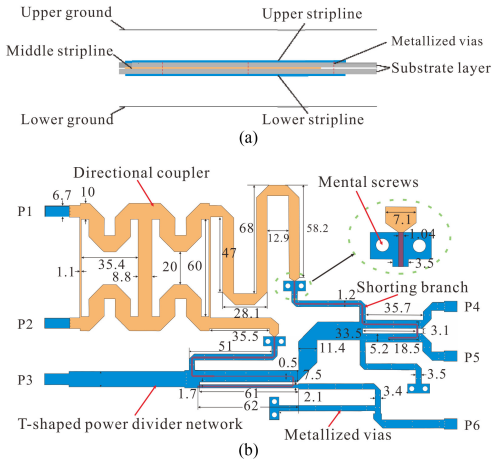


Fig. 3. (a) Cross-sectional view. (b) Configuration of the proposed BM.

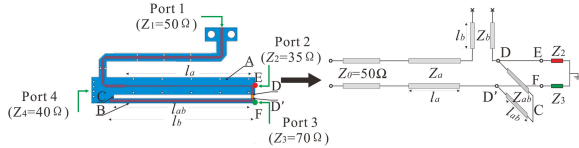
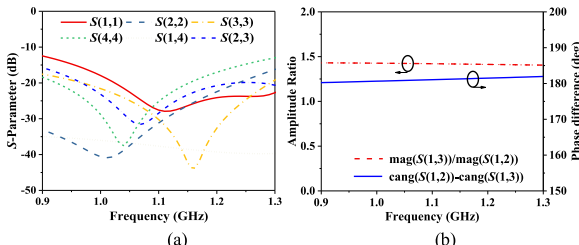


Fig. 4. Construction and equivalent circuit of the 1.77 dB coupling balun.

Fig. 5. Simulated results of the 1.77 dB coupling balun. (a). S -parameter. (b). Amplitude ratio and phase difference of the output ports.

different directions can be generated to achieve a typical 2-D beamforming property.

A. Theoretical Analysis of the Three-Beam BM

In this section, a novel topology of the three-beam BM is proposed, as shown in Fig. 2. It mainly comprises three simple components: a directional coupler, T-shaped power dividers, and coupling baluns. To explain the working mechanism of the matrix, a transmission matrix is analyzed as follows.

The transmission matrices of directional couplers, T-shaped power dividers, and coupling baluns are denoted as C , T , and B , respectively. In the BM network, two power ratios are designed:

1:1 and 1:2. The phase delays between outports for the above-mentioned three components are 90° , 0° , and 180° , respectively. The transmission matrices of the five components in Fig. 2 are expressed as follows:

$$C = \begin{bmatrix} \frac{1}{\sqrt{2}} & -j\frac{1}{\sqrt{2}} \\ -j\frac{1}{\sqrt{2}} & \frac{1}{\sqrt{2}} \end{bmatrix}, T_1 = \begin{bmatrix} \frac{\sqrt{2}}{\sqrt{3}} & \frac{1}{\sqrt{3}} \\ \frac{1}{\sqrt{3}} & \frac{1}{\sqrt{2}} \end{bmatrix}, T_2 = \begin{bmatrix} \frac{1}{\sqrt{2}} & \frac{1}{\sqrt{2}} \\ j\frac{1}{\sqrt{2}} & -j\frac{1}{\sqrt{3}} \end{bmatrix}$$

$$B_1 = \begin{bmatrix} j\frac{1}{\sqrt{3}} & -j\frac{1}{\sqrt{3}} \end{bmatrix}, B_2 = \begin{bmatrix} j\frac{1}{\sqrt{2}} & -j\frac{1}{\sqrt{2}} \end{bmatrix}. \quad (1)$$

The transmission of the entire three-beam BM can be divided into three parts corresponding to three transmission matrices: Q_1 , Q_2 , and Q_3 . Considering the continuous transmission of signals, the transmission matrix of the entire BM network can be expressed as follows:

$$Q = Q_1 Q_2 Q_3 = \begin{bmatrix} C & & \\ & 1 & \\ & & T_1 \end{bmatrix} \begin{bmatrix} 1 & & \\ B_2 & & \\ T_2 & & 1 \end{bmatrix} = \frac{1}{\sqrt{3}} \begin{bmatrix} e^{j\frac{\pi}{3}} & e^{-j\frac{\pi}{3}} & e^{-j\pi} \\ e^{j\frac{\pi}{6}} & e^{j\frac{5\pi}{6}} & e^{-j\frac{\pi}{4}} \\ 1 & 1 & 1 \end{bmatrix}. \quad (2)$$

From matrix Q , the coefficient of the transmission matrix is $1/\sqrt{3}$, and the phase difference of each row is $-2\pi/3$, $2\pi/3$, and 0 . These results indicate that the proposed topology can allocate desired output signals of equal magnitude and linear phase delay, which is consistent with the output characteristics of the proposed three-beam BM.

B. Realization of the Three-Beam BM

The detailed configuration of the three-beam BM is shown in Fig. 3. The network is fabricated on a middle double-layer Rogers 5880 substrate ($\epsilon_r = 2.2$ and $\tan \delta = 0.0009$) with a thickness of 1.574 mm. The entire BM network is placed in a closed metal cavity, and six SMA connectors are set on the sidewalls corresponding to the input and output terminals on the upper layer of the double-layer substrate.

The structure and dimensions of the BM network are shown in Fig. 3(b). A dual-stripline structure is introduced to achieve size reduction by combining multiple components. First, a three-dB branch directional coupler set at the center of the double-layer substrate and a T-shaped power divider network arranged on both sides of the double-layer substrate are used as the inner cores and combined with the upper and lower grounds to form the first stage stripline. In addition, the double-layer T-shaped power divider network with short metallized vias acts as the outer conductor of the second-stage stripline structure. The two output lines of the three-dB branch directional coupler [see thin red lines in Fig. 3(b)] are transformed into a T-shaped power divider network as the inner core of the second-stage stripline. To provide an efficient connection channel for the dual-stripline, four quarter wavelength branches are introduced with eight shorting metal screws to the T-shaped power divider network. In this case, the second-stage stripline constitutes two coupling baluns, i.e., 1.77 dB and 3 dB.

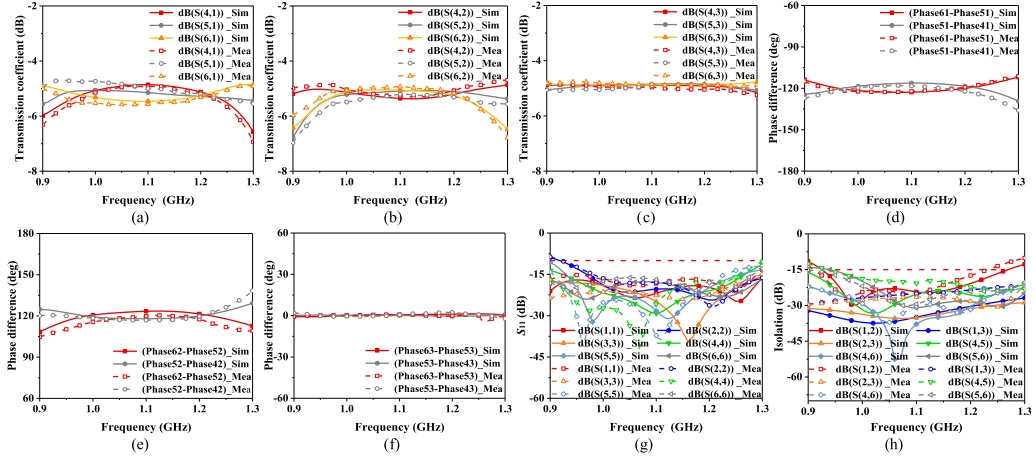


Fig. 6. Simulation and measurement results of the proposed BM. (a)–(c) Transmission coefficient. (d)–(f) Phase difference. (g) Reflection coefficient. (h) Isolation.

To illustrate the working principle, the circuit of the 1.77 dB coupling balun is analyzed. Its structure and equivalent circuit diagram are shown in Fig. 4. Unlike the traditional baluns used for antenna feeds [26], [27], for the coupling balun, the output impedances R_1 and R_2 in series represent the input impedances of the subsequent transmission lines. The power distribution ratio of ports E and F is K ($K = R_1 : R_2 = 1 : 2$ for the 1.77 dB coupling balun). The coupling balun can be regarded as a four-port network, where port 1 is the input port, ports 2 and 3 are the output ports, and port 4 is the isolation port. The simulated results in Fig. 5 exhibit the simulated return loss at the input and output ports, where the 10 dB bandwidth is 0.6 GHz (54.1%). In our focus bandwidth (0.9–1.3 GHz), the isolations between the ports are greater than 15 dB (ports 2 and 3) and 35 dB (ports 1 and 4). The phase difference between the output ports is 180° , and the phase fluctuation is less than 2° . The amplitude ratio of the output port ranges from 1.4 to 1.43, indicating a power division of 1:2. These results indicate that the introduction of the coupling balun can play a role in both power distribution and phase shift.

When port 1 or 2 is excited, the signals are first distributed by the 3 dB branch directional coupler and then fed into the second-stage stripline. Finally, the signals processed by the two baluns reach three output ports for signal synthesis. When port 3 is excited, only the T-shaped power divider network is used to achieve equal power and phase signal outputs. The simulated results of the corresponding S -parameters are shown in Fig. 6.

In summary, the circuit topology in Fig. 2 is realized intelligently. The reuse of spaces and routes effectively reduced the network size. The circuit size was only $153 \times 256 \text{ mm}^2$ ($0.56 \times 0.94 \lambda^2$, where λ is the free-space wavelength at 1.1 GHz).

C. Two-Dimensional Scanning Multibeam Array

To verify the function of the 2-D BFN, a 3×3 half-mode microstrip array antenna is designed. The dimensions and configuration of the array elements are depicted in Fig. 7(a). The antenna comprises two half-mode microstrip antennas shortened on one side, a feed probe with disk loading, and a metal ground. Two pairs of shorting pins are introduced on each side of the two microstrip patches to reduce the cross-polarized radiation

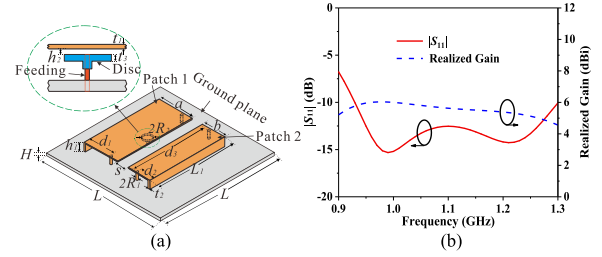


Fig. 7. (a) Geometry and (b) simulated results of the antenna unit. $a = 75$, $b = 49$, $s = 21$, $d_1 = 53.5$, $d_2 = 32.5$, $d_3 = 157$, $L_1 = 165$, $L = 250$, $t_1 = 2 \text{ mm}$, $t_2 = 4 \text{ mm}$, $t_3 = 3 \text{ mm}$, $R_1 = 5$, $R_2 = 9.75$, $h_1 = 17.5$, $h_2 = 2.5$, and $H = 5$. Unit: mm.

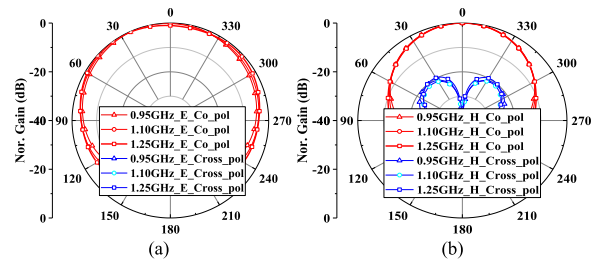


Fig. 8. Simulated radiation pattern at 0.95, 1.1, and 1.25 GHz for the antenna element. (a) E -plane. (b) H -plane.

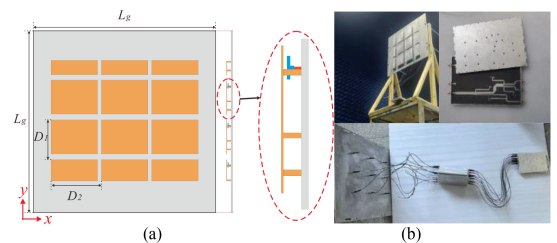


Fig. 9. (a) Configuration of the nine-element antenna array. (b) Test environment and overall structure.

and simultaneously act as support columns [28]. Fig. 7(b) shows that a wide bandwidth ($|S_{11}| < -10 \text{ dB}$) of 34.5% covering 0.93–1.31 GHz and two attenuation poles (1.0 and 1.21 GHz) are achieved. In addition, a stable normal radiation pattern with identical polarization, wide half-power beamwidth (HPBW) (154° in the E -plane), and low cross-polarization properties

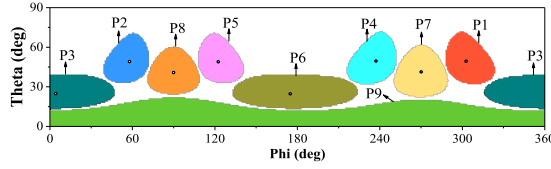


Fig. 10. Simulated 2-D radiation patterns.

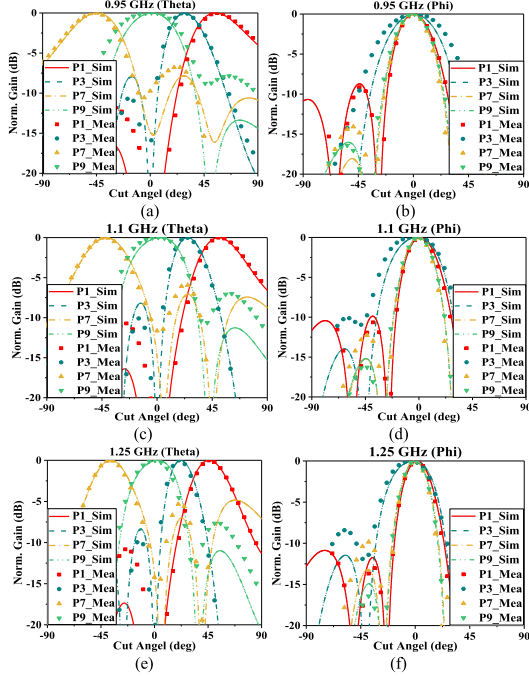


Fig. 11. Simulated and measured radiation pattern of the array patterns on the Theta and Phi tangent planes. (a) 0.95 GHz, Theta. (b) 0.95 GHz, Phi. (c) 1.1 GHz, Theta. (d) 1.1 GHz, Phi. (e) 1.25 GHz, Theta. (f) 1.25 GHz, Phi.

(<-16 dB) are successfully achieved in the entire operation band shown in Fig. 8.

Based on the proposed antenna unit, a 3×3 array antenna is developed, as shown in Fig. 9(a). The distance between the adjacent elements is $D_1 = 141$ mm and $D_2 = 180$ mm. By adding the corresponding excitation signal, nine beams with different directions were generated (see Fig. 10).

III. EXPERIMENTAL RESULTS

To verify the theoretical results, the proposed three-beam BM is initially fabricated, as depicted in Fig. 9(b). The S-parameters of the BFN are measured using an AV3672B vector network analyzer (see Fig. 6). In the operation bandwidth (0.95–1.25 GHz for 12 dB return loss), the transmission coefficient is approximately -5.2 dB, and the phase delays are approximately -120° , 120° , and 0° . In the entire operation bandwidth, a 0.7 dB variation in the transmission coefficient and a $\pm 5^\circ$ variation in the output phase are achieved under P1–P9 excitations. In addition, the isolations between each pair of input and output ports are >14 dB. The measured results agree well with the simulation and theoretical results. Table I shows the comparison between the three-beam BFNs obtained in this article and other previous works. The beam-forming network in this letter has excellent performance, including the lowest loss, wide operating bandwidth, and lower output amplitude and phase fluctuations.

TABEL I
COMPARISON BETWEEN THE PROPOSED THREE-BEAM BM WITH OTHER BFNs

Performance	[15]	[17]	[9]	[3]	Our work
Type	Stripline		Microstrip		Stripline
Size (λ)	NG	NG	1.38×0.61	NG	0.94×0.56
Layer	3	3	1	2	2
Imbalance (M/P)	1.2 dB $\pm 10^\circ$	0.6 dB $\pm 3^\circ$	0.4 dB $\pm 4.1^\circ$	2.6 dB $\pm 10^\circ$	0.7 dB $\pm 5^\circ$
IL(dB)	0.5–1.5	>1	NG	1–2.4	0.3–1.4
BW (RL > 10 dB)	46%	33%	8%	7%	34.5%
Antenna realization	Yes	No	Yes	Yes	Yes

NG: not given; M/P: magnitude/phase; IL: insertion loss RL: return loss; BW: bandwidth.

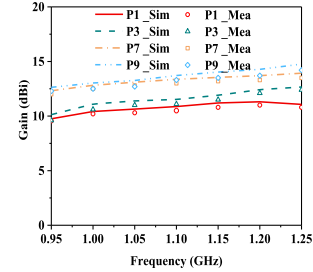


Fig. 12. Simulated and measured gain of the array patterns corresponding to ports 1, 3, 7, and 9.

In addition, the compact structure and fewer layers are implemented simultaneously.

Finally, the proposed 2-D scanning phased-array antenna is fabricated, assembled, and tested. Fig. 9(b) depicts the array and test environment. A near-field SATIMO antenna test system is employed to test the radiation pattern of the array. Based on the symmetric relation, the simulated and measured radiation patterns corresponding to ports 1, 3, 7, and 9 are shown in Fig. 11, which indicates that the beam direction of the array agrees with the simulation. The results demonstrate that nine beams with different spatial orientations are realized with the excitation of nine ports. The measured and simulated gain of the antenna array are shown in Fig. 12. The variation trend of the measured gain with frequency is consistent with the simulated results. However, the problem of sidelobe level elevation, beam broadening, and gain reduction occur, mainly because of the array antenna installation error, especially the unit phase error.

IV. CONCLUSION

In this letter, a broadband 2-D scanning multibeam array antenna using a novel BFN is presented. First, a three-beam BM is theoretically analyzed as the core component. To avoid the introduction of complex crossovers and lossy lumped elements, a dual stripline structure is employed, and the circuit structure is realized using only the conventional broadband directional coupler, T-shaped power dividers, and coupling baluns. Then, six three-beam BFs are interconnected to construct a nine-beam 2-D BFN. Finally, a wideband low-profile half-mode microstrip antenna is designed to form a 3×3 antenna array, which is combined with the BFN to realize beam scanning in nine directions. The antenna is a good candidate for 2-D scanning because of its compact structure, low cost, and flexible beam.

REFERENCES

- [1] Y. Li and K.-M. Luk, "A multibeam end-fire magnetoelectric dipole antenna array for millimeter-wave applications," *IEEE Trans. Antennas Propag.*, vol. 64, no. 7, pp. 2894–2904, Jul. 2016.
- [2] J.-W. Lian, Y.-L. Ban, J.-Q. Zhu, K. Kang, and Z. P. Nie, "Compact 2-D scanning multibeam array utilizing the SIW three-way couplers at 28 GHz," *IEEE Antennas Wireless Propag. Lett.*, vol. 17, no. 10, pp. 1915–1919, Oct. 2018.
- [3] K. Ding, X. Fang, Y. Wang, and A. Chen, "Printed dual-layer three way directional coupler utilized as 3×3 beamforming network for orthogonal three-beam antenna array," *IEEE Antennas Wireless Propag. Lett.*, vol. 13, pp. 911–914, 2014.
- [4] J. Blass, "Multidirectional antenna—A new approach to stacked beams," in *Proc. IRE Int. Conf. Rec.*, 1960, pp. 48–50.
- [5] S. Mosca, F. Bilotti, A. Toscano, and L. Vigni, "A novel design method for blass matrix beam-forming networks," *IEEE Trans. Antennas Propag.*, vol. 50, no. 2, pp. 225–232, Feb. 2002.
- [6] C. Tokos *et al.*, "Analysis of a multibeam optical beamforming network based on blass matrix architecture," *J. Lightw. Technol.*, vol. 36, no. 15, pp. 3354–3372, Aug. 2018.
- [7] T. Djerafi, N. J. G. Fonseca, and K. Wu, "Planar Ku-band 4×4 nolen matrix in SIW technology," *IEEE Trans. Microw. Theory Techn.*, vol. 58, no. 2, pp. 259–266, Feb. 2010.
- [8] T. Djerafi, N. J. G. Fonseca, and K. Wu, "Broadband substrate integrated waveguide 4×4 nolen matrix based on coupler delay compensation," *IEEE Trans. Microw. Theory Techn.*, vol. 59, no. 7, pp. 1740–1745, Jul. 2011.
- [9] H. Ren, H.-X. Zhang, Y.-Q. Jin, Y.-X. Guo, and B. Arigong, "A novel 2-D 3×3 nolen matrix for 2-D beamforming applications," *IEEE Trans. Microw. Theory Techn.*, vol. 67, no. 11, pp. 4622–4631, Nov. 2019.
- [10] J. Butler and R. Lowe, "Beam forming matrix simplifies design of electronically scanned antennas," *Electron. Des.*, vol. 9, pp. 170–173, Apr. 1961.
- [11] C. Liu, S. Xiao, Y.-X. Guo, Y.-Y. Bai, and B.-Z. Wang, "Broadband circularly polarized beam-steering antenna array," *IEEE Trans. Antennas Propag.*, vol. 61, no. 3, pp. 1475–1479, Mar. 2013.
- [12] E. Gandini, M. Ettorre, R. Sauleau, and A. Grbic, "A lumped-element unit cell for beam forming networks and its application to a miniaturized butler matrix," *IEEE Trans. Microw. Theory Techn.*, vol. 61, no. 4, pp. 1477–1487, Apr. 2013.
- [13] H. Ren, B. Arigong, M. Zhou, J. Ding, and H.-L. Zhang, "A novel design of 4×4 butler matrix with relatively flexible phase differences," *IEEE Antennas Wireless Propag. Lett.*, vol. 15, pp. 1277–1280, 2016.
- [14] C.-C. Chang, R.-H. Lee, and T.-Y. Shih, "Design of a beam switching/steering butler matrix for phased array system," *IEEE Trans. Antennas Propag.*, vol. 58, no. 2, pp. 367–374, Feb. 2010.
- [15] H. Zhu, H.-H. Sun, B. Jones, C. Ding, and Y. J. Gu, "Wideband dual-polarized multiple beam-forming antenna arrays," *IEEE Trans. Antennas Propag.*, vol. 67, no. 3, pp. 1590–1604, Mar. 2019.
- [16] H. Zhu, H. H. Sun, C. Ding, and Y. J. Guo, "Butler matrix based multi-beam base station antenna array," in *Proc. 13th Eur. Conf. Antennas Propag.*, 2019, pp. 1–4.
- [17] S. Odrobina, K. Staszek, K. Wincza, and S. Gruszczynski, "Broadband 3×3 butler matrix," in *Proc. Conf. Microw. Techn.*, 2017, pp. 1–5.
- [18] K. Tekkouk, J. Hirokawa, R. Sauleau, M. Ettorre, M. Sano, and M. Ando, "Dual-layer ridged waveguide slot array fed by a butler matrix with sidelobe control in the 60-GHz band," *IEEE Trans. Antennas Propag.*, vol. 63, no. 9, pp. 3857–3867, Sep. 2015.
- [19] S. Karamzadeh, V. Rafii, M. Kartal, and B. S. Virdee, "Compact and broadband 4×4 SIW butler matrix with phase and magnitude error reduction," *IEEE Microw. Wireless Compon. Lett.*, vol. 25, no. 12, pp. 772–774, Dec. 2015.
- [20] W. F. Moulder, W. Khalil, and J. L. Volakis, "60-GHz two-dimensionally scanning array employing wideband planar switched beam network," *IEEE Antennas Wireless Propag. Lett.*, vol. 9, pp. 818–821, 2010.
- [21] W. Yang, Y. Yang, W.-Q. Che, C. Fan, and Q. Xue, "94-GHz compact 2-D multibeam LTCC antenna based on multifolded SIW beam-forming network," *IEEE Trans. Antennas Propag.*, vol. 65, no. 8, pp. 4328–4333, Aug. 2017.
- [22] J.-X. Wang, Y.-J. Li, L. Ge, W. J.-H., and K. M. Luk, "A 60 GHz horizontally polarized magnetoelectric dipole antenna array with 2-D multibeam endfire radiation," *IEEE Trans. Antennas Propag.*, vol. 65, no. 11, pp. 5837–5846, Nov. 2017.
- [23] A. B. Guntupalli, T. Djerafi, and K. Wu, "Two-dimensional scanning antenna array driven by integrated waveguide phase shifter," *IEEE Trans. Antennas Propag.*, vol. 62, no. 3, pp. 1117–1124, Mar. 2014.
- [24] J.-W. Lian, Y.-L. Ban, Q.-L. Yang, B. Fu, Z.-F. Yu, and L.-K. Sun, "Planar millimeter-wave 2-D beam-scanning multibeam array antenna fed by compact SIW beam-forming network," *IEEE Trans. Antennas Propag.*, vol. 66, no. 3, pp. 1299–1310, Mar. 2018.
- [25] J.-W. Lian, H. Zhu, Y.-L. Ban, D. K. Karmokar, and Y. J. Guo, "Uniplanar high-gain 2-D scanning leaky-wave multibeam array antenna at fixed frequency," *IEEE Trans. Antennas Propag.*, vol. 68, no. 7, pp. 5257–5268, Jul. 2020.
- [26] R. Bawer and J. J. Wolfe, "A printed circuit balun for use with spiral antennas," *IRE Trans. Microw. Theory Tech.*, vol. 8, no. 3, pp. 319–325, May 1960.
- [27] Z. W. Zhou, S. W. Yang, and Z. P. Nie, "A novel broadband printed dipole antenna with low cross-polarization," *IEEE Trans. Antennas Propag.*, vol. 55, no. 11, pp. 3091–3093, Nov. 2007.
- [28] N.-W. Liu, Sun M.-Jiao, L. Zhu, D.-P. Xie, and G. Fu, "A low-profile printed cavity antenna with simultaneous bandwidth and radiation pattern improvement," *IEEE Antennas Wireless Propag. Lett.*, vol. 18, no. 10, pp. 2125–2129, Oct. 2019.